Experimental realization of high-fidelity teleportation via a non-Markovian open quantum system

Zhao-Di Liu,[1,2] Yong-Nan Sun,[1,2] Bi-Heng Liu,[1,2] Chuan-Feng Li,[1,2,*] Guang-Can Guo,[1,2]
Sina Hamedani Raja,[3] Henri Lyyra,[3,4] and Jyrki Piilo[3,†]

[1]*CAS Key Laboratory of Quantum Information, University of Science and Technology of China, Hefei 230026, China*
[2]*CAS Center For Excellence in Quantum Information and Quantum Physics, University of Science and Technology of China, Hefei 230026, China*
[3]*Turku Centre for Quantum Physics, Department of Physics and Astronomy, University of Turku, FI-20014 Turun yliopisto, Finland*
[4]*Department of Physics and Nanoscience Center, University of Jyväskylä, FI-40014 University of Jyväskylä, Finland*

(Received 2 July 2020; accepted 17 November 2020; published 11 December 2020)

Open quantum systems and study of decoherence are important for our fundamental understanding of quantum physical phenomena. For practical purposes, a large number of quantum protocols exist that exploit quantum resources, e.g., entanglement, which allows us to go beyond what is possible to achieve by classical means. We combine concepts from open quantum systems and quantum information science and give a proof-of-principle experimental demonstration—with teleportation—that it is possible to implement efficiently a quantum protocol via a non-Markovian open system. The results show that, at the time of implementation of the protocol, it is not necessary to have the quantum resource in the degree of freedom used for the basic protocol—as long as there exists some other degree of freedom or the environment of an open system, which contains useful resources. The experiment is based on a pair of photons, where their polarizations act as open system qubits and frequencies as their environments, while the path degree of freedom of one of the photons represents the state of Alice's qubit to be teleported to Bob's polarization qubit.

DOI: 10.1103/PhysRevA.102.062208

I. INTRODUCTION

The study of open quantum systems is important for both fundamental and practical purposes. When an open system interacts with its environment, this typically leads to decoherence and loss of quantum properties [1,2], which, in turn,often makes it difficult to implement quantum protocols in an ideal manner in experiments [3]. In general, during the last 10 years, there have been significant developments in understanding and characterizing the abundant and diverse features of open system dynamics [4–9]. These developments have influenced, and have been influenced by, the increasing ability to realize experimentally reservoir engineering [10], various fundamental open system models in non-Markovian regimes [11], and the control of open system dynamics [12]. Indeed, a number of various physical platforms have been used for this purpose including, e.g., optical systems [11–21], NV centers [22,23], trapped ions [24], and NMR systems [25,26]. In addition to fundamental studies and tests, recent experimental work also includes some of the first exploitations of non-Markovian memory effects in basic quantum information protocols including, e.g., single-qubit Deutsch-Josza algorithm [27].

Considering entanglement, as a matter of fact, it plays a dual role when considering implementation of quantum protocols with systems interacting with their environments. To start with, we need entanglement—as a quantum resource—when implementing quantum protocols and to go beyond what can be achieved by classical resources. However, when an open system interacts with its environment, the entanglement within the open system decreases due to decoherence, and the efficiency of the quantum protocol typically diminishes. At the same time, the open system often gets entangled with its environment. This means that the total system-environment state still contains a useful resource, while it no longer resides in the degrees of freedom which are explicitly used for the implementation of the quantum protocol.

Therefore, we arrive at the following question: Is it possible to efficiently realize a quantum information protocol experimentally via an open quantum system? We answer this question affirmatively and demonstrate a proof-of-principle experiment by using teleportation [28] as an example. This also means that we combine the central concepts of quantum information and open quantum systems in a new fundamental manner in an experiment. Note that for technological purposes, there have recently been impressive experiments, e.g., demonstrating ground-to-satellite teleportation [29] and superdense teleportation for information transfer using a pair of hyperentangled photons [30]. We, instead, see our current contribution dealing with fundamental questions on open quantum systems and quantum information. Our experiment uses the concept of nonlocal memory effects [14,17,31] and a recent theoretical proposal of how to exploit them in teleportation [32]. For completeness, we next recall the basic steps of the scheme, including some changes compared to the original theoretical proposal, and then continue to the experimental section and results.

*cfli@ustc.edu.cn
†jyrki.piilo@utu.fi

II. THEORETICAL DESCRIPTION

First, we prepare a polarization entangled state $|\phi^+\rangle_{ab} = \frac{1}{\sqrt{2}}(|HH\rangle + |VV\rangle)$, where $H(V)$ denotes the horizontal (vertical) polarization of the photon. The total initial polarization-frequency two-photon state is

$$|\psi(0)\rangle = |\phi^+\rangle_{ab} \otimes \int d\omega_a d\omega_b g(\omega_a, \omega_b) |\omega_a\rangle |\omega_b\rangle, \quad (1)$$

where $g(\omega_a, \omega_b)$ is the joint frequency amplitude distribution of photons a and b with $\int d\omega_a d\omega_b |g(\omega_a, \omega_b)|^2 = 1$. We describe below in more detail what role the properties of $|g(\omega_a, \omega_b)|^2$ play in the protocol. Before Alice receives her photon, its polarization and frequency are coupled in a quartz plate. This local interaction is given by the time-evolution operator

$$U(t)|\lambda\rangle|\omega\rangle = \exp(in_\lambda \omega t)|\lambda\rangle|\omega\rangle, \quad (2)$$

where λ denotes the given polarization direction and n_λ its index of refraction in the quartz plate. Even though the polarization-frequency state remains pure, this leads to dephasing of the polarization degree of freedom [11,14]. Indeed, after the local interaction in the side of Alice, the two-photon polarization-frequency state is both pure and entangled,

$$|\psi(t_a)\rangle = \frac{1}{\sqrt{2}}(|HH\rangle |\xi_{HH}(t_a)\rangle + |VV\rangle |\xi_{VV}(t_a)\rangle), \quad (3)$$

where $|\xi_{\lambda\lambda}(t_a)\rangle = \int d\omega_a d\omega_b g(\omega_a, \omega_b) e^{in_\lambda^a \omega_a t_a} |\omega_a\rangle |\omega_b\rangle$. The joint polarization state, in turn, is no longer fully entangled and has become a mixed state,

$$\rho_{ab}(t_a) = \tfrac{1}{2}(|HH\rangle\langle HH| + \kappa_1(t_a)|HH\rangle\langle VV| + \kappa_1^*(t_a)|VV\rangle\langle HH| + |VV\rangle\langle VV|), \quad (4)$$

where the local decoherence function is

$$\kappa_a(t_a) = \int d\omega_a d\omega_b |g(\omega_a, \omega_b)|^2 e^{-i\Delta n_a \omega_a t_a}, \quad (5)$$

with $\Delta n_a = n_V^a - n_H^a$.

Alice prepares now a third qubit in the state which she wants to teleport to Bob. Unlike the original proposal, where a third photon is used for this purpose [32], she introduces a binary path degree of freedom of the photon she possesses. In general this path qubit state is $|\phi\rangle_s = \alpha|0\rangle + \beta|1\rangle$, where $|0\rangle$ and $|1\rangle$ denote the two spatial paths she uses. Therefore, Alice's and Bob's overall state is now $|\Psi(t_a)\rangle = \frac{1}{\sqrt{2}}|\phi\rangle_s [(|HH\rangle |\xi_{HH}(t_a)\rangle + |VV\rangle |\xi_{VV}(t_a)\rangle]$. We can now write this state by using the Bell-state basis of the two qubits of Alice and obtain

$$\begin{aligned}|\Psi(t_a)\rangle = {} & \tfrac{1}{2}|\Phi^+\rangle_{sa}[\alpha|H\rangle_b|\xi_{HH}(t_a)\rangle + \beta|V\rangle_b|\xi_{VV}(t_a)\rangle] \\ & + \tfrac{1}{2}|\Phi^-\rangle_{sa}[\alpha|H\rangle_b|\xi_{HH}(t_a)\rangle - \beta|V\rangle_b|\xi_{VV}(t_a)\rangle] \\ & + \tfrac{1}{2}|\Psi^+\rangle_{sa}[\beta|H\rangle_b|\xi_{HH}(t_a)\rangle + \alpha|V\rangle_b|\xi_{VV}(t_a)\rangle] \\ & + \tfrac{1}{2}|\Psi^-\rangle_{sa}[\alpha|V\rangle_b|\xi_{VV}(t_a)\rangle - \beta|H\rangle_b|\xi_{HH}(t_a)\rangle], \end{aligned} \quad (6)$$

where $|\Phi^\pm\rangle_{sa} = \frac{1}{\sqrt{2}}(|0\rangle|H\rangle \pm |1\rangle|V\rangle)$ and $|\Psi^\pm\rangle_{sa} = \frac{1}{\sqrt{2}}(|0\rangle|V\rangle \pm |1\rangle|H\rangle)$. It is noteworthy that in each line—corresponding to four outcomes of Alice's measurement—we have a pure and entangled state between Bob's polarization and the frequencies of the two photons, in addition to the amplitudes α and β being transferred.

Alice communicates her measurement result to Bob. What should he do now? Bob first applies one of the four unitary transformations on his qubit—according to the standard teleportation scheme—and then applies local polarization-frequency dephasing interaction to his photon. The cases corresponding to four outcomes for Alice are (i) $|\Phi^+\rangle_{sa} \Rightarrow \mathbb{I}$, $\Delta n_b = \Delta n_a$; (ii) $|\Phi^-\rangle_{sa} \Rightarrow \sigma_z$, $\Delta n_b = \Delta n_a$; (iii) $|\Psi^+\rangle_{sa} \Rightarrow \sigma_x$, $\Delta n_b = -\Delta n_a$; and (iv) $|\Psi^-\rangle_{sa} \Rightarrow i\sigma_y$, $\Delta n_b = -\Delta n_a$. Here, σ_x, σ_y, and σ_z are the unitary Pauli rotations, and Δn_b indicates the conditional choice for Bob's birefringence. Let us, as an example, check one of the four cases in detail.

Suppose that Alice's measurement outcome was $|\Phi^+\rangle_{sa}$, corresponding to the first line of Eq. (6). For this case, Bob's unitary qubit transformation is the identity operator and he only needs to apply dephasing noise with $\Delta n_b = \Delta n_a$. Once Bob applies the dephasing interaction for the duration t_b, the state of his polarization qubit is

$$\begin{aligned}\rho_b = {} & |\alpha|^2 |H\rangle\langle H| + \alpha\beta^*\kappa(t_a, t_b)|H\rangle\langle V| \\ & + \alpha^*\beta\kappa^*(t_a, t_b)|V\rangle\langle H| + |\beta|^2|V\rangle\langle V|, \end{aligned} \quad (7)$$

where the decoherence function $\kappa(t_a, t_b)$ is given by

$$\kappa(t_a, t_b) = \int d\omega_a d\omega_b |g(\omega_a, \omega_b)|^2 e^{-i\Delta n_b(\omega_a t_a + \omega_b t_b)}. \quad (8)$$

Note that the photon on the side of Alice is already destroyed. However, the influence of Bob's local noise on his polarization state does depend on the initial joint two-photon frequency distribution $|g(\omega_a, \omega_b)|^2$.

The question now becomes whether it is possible to have $|\kappa(t_a, t_b)| = 1$ so that Bob eventually has a pure polarization state after his noise, while at all of the previous points in the protocol the state has been mixed. For this purpose, let us study the properties of the initial two-photon frequency distribution $|g(\omega_a, \omega_b)|^2$.

We consider the joint two-photon frequency distribution $|g(\omega_a, \omega_b)|^2$ in a downconversion process as a bivariate Gaussian distribution [14,31] with covariance matrix elements $C_{ij} = \langle\omega_i\omega_j\rangle - \langle\omega_i\rangle\langle\omega_j\rangle$. The means and variances for the two photons are $\langle\omega_a\rangle = \langle\omega_b\rangle = \omega_0/2$, where ω_0 is the frequency of the downconversion pump, and $C_{11} = C_{22} = \langle\omega_i^2\rangle - \langle\omega_i\rangle^2$. The frequency-frequency correlation is quantified by the coefficient $K = C_{11}/\sqrt{C_{11}C_{22}} = C_{12}/C_{11}$, such that $|K| \leqslant 1$. Taking initially a maximally anticorrelated frequency distribution with $K = -1$ having $\omega_a + \omega_b = \omega_0$, and Bob's using interaction time $t_b = t_a$, the magnitude of his decoherence function becomes $|\kappa(t_a, t_b)| = 1$, and after applying the local noise he obtains the pure polarization state,

$$|\psi_F\rangle = \alpha|H\rangle + \beta e^{i\omega_0 \Delta n_b t_b}|V\rangle. \quad (9)$$

Bob can, in a straightforward manner, cancel the extra relative phase with ω_0 and, therefore, succeed in teleportation with a fidelity equal to 1. Note that in general for dephasing, the width of the single-peak Gaussian frequency distribution defines how strongly the exponential damping of the magnitude of the decoherence function occurs—when there is a single photon or noise only on one side of the two-photon system

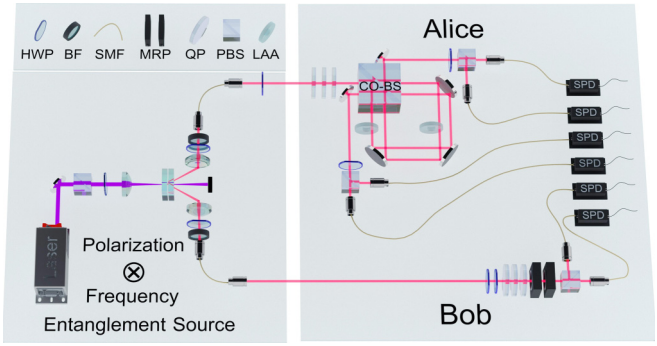

FIG. 1. Experimental setup. The two-photon state is prepared by spontaneous parametric downconversion (SPDC) pumping of the β-barium-borate (BBO) crystal with a continuous-wave (CW) laser. The BFs are used to choose the photons. QPs implement the noise on Alice's side. To prepare Alice's path qubit state and to prepare for path qubit Bell measurement, a specifically designed Sagnac interference ring of a very high stability is used. Here, we use a combined beam splitter (CO-BS), which consists of a beam splitter and polarizing beam splitter parts. The path qubit state itself is prepared with LAAs along the paths inside the interferometer. Alice's HWPs, PBSs. and SPDs complete the Bell measurement. On Bob's side, HWPs induce unitary transformation, QPs induce dephasing noise, and state tomography is performed with MRP, PBS, and SPDs. HWP, half-wave plate; BF, bandpass filter; SMF, single-mode fiber; MRP, motor rotating plate; QP, quartz plate; PBS, polarizing beam splitter; LAA, linear adjustable attenuator; SPD, single-photon detector.

destroying the polarization entanglement (see, e.g., Ref. [11]). In the ideal case described in Eq. (9), both photons still have finite local frequency distribution widths (C_{11} and C_{22}) and subsequent sources of dephasing even though the final teleported state can be a pure state because $K = -1$.

III. EXPERIMENTAL SETUP

We display the experimental setup in Fig. 1. To prepare the required initial state, we exploit an SPDC process where a 404-nm CW laser pumps a BBO crystal. This crystal is made of two orthogonal glued type I phase-matched BBOs and can be used to produce polarization entangled photons by using the $H + V$ direction polarized laser pump. The frequency correlations, in turn, arise due to the narrow linewidth of the CW pump laser. In our case, the 404-nm pump has a measured linewidth below 0.06 nm. After downconversion, the photons have a bandwidth of the order of 135 nm. Then 3-nm-FWHM (full width at half-maximum) bandpass filters (centered at 808 nm) are used to choose the most indistinguishable SPDC photon pairs. Even though the filtering changes the frequency distribution, there is still a large amount of frequency-frequency correlations left due to the very narrow pump linewidth. Note also that in the 3-nm frequency window used, the difference in the indices of refraction for ordinary vs extraordinary rays can be considered constant at a value of 0.00889.

On Alice's side, we first insert quartz plates, of increasing thickness corresponding to increasing interaction times, to induce dephasing noise for Alice's polarization qubit. Then Alice prepares her path qubit to be teleported and makes the polarization-path Bell measurement. Earlier proposals for path-polarization measurement have used, e.g., the Mach-Zehnder interferometer [33]. However, to significantly improve the stability of the scheme required for teleportation, we have designed a specific Sagnac interferometer for this purpose. Here, the crucial component is a specific beam splitter (CO-BS) which consists of half BS and half PBS. When the photon enters the Sagnac interferometer, it goes through the BS part of the CO-BS. Along the paths of the interferometer, there are LAAs that produce an arbitrary ratio of the two paths and prepare the path qubit state to be teleported. Note that the path degree of freedom is completely independent of the polarization and frequency degrees of freedom of the photon. Alice can then make the Bell measurement by interfering her two paths, when the photon exits the interferometer in the PBS part of the CO-BS, and by using other PBSs at 45° at each output path before the photon hits the SPDs at the outputs.

On Bob's side, he first implements with HWP the unitary operation on his polarization qubit based on Alice's Bell measurement outcome. Next, he induces dephasing noise by using quartz plates to couple the polarization (open system) and frequency (environment). Finally, using MRPs and PBS, he performs state tomography of his qubit and completes the protocol.

IV. RESULTS

We now present two sets of experimental results. In both cases, the success of the teleportation is quantified in the usual manner by fidelity $F(\rho_{\rm out}, \rho_{\rm in}) = (\mathrm{tr}\sqrt{\sqrt{\rho_{\rm out}}\rho_{\rm in}\sqrt{\rho_{\rm out}}})^2$ between the state Alice prepared, $\rho_{\rm in}$, and the state Bob measured after completing the protocol, $\rho_{\rm out}$.

Alice's qubit resides in the path degree of freedom of the photon, while Bob's qubit corresponds to the polarization state of another photon. Note that the maximum fidelity with fully classical mixed states and using LOCC is 2/3 [34]. The results are presented for all four possible Bell-state measurement outcomes for Alice $\{|\Phi^+\rangle, |\Phi^-\rangle, |\Psi^+\rangle, |\Psi^-\rangle\}$.

In the first part of the first experiment, the duration of the noise t_a on Alice's side is increased in a stepwise manner before her Bell measurement. She has prepared the path qubit state to be teleported, which, based on the experimental state tomography, is given by

$$\rho_+ = \begin{pmatrix} 0.5507 & 0.4871 + i0.1007 \\ 0.4871 - i0.1007 & 0.4492 \end{pmatrix}. \quad (10)$$

This is expressed in the path qubit basis $|0\rangle$ and $|1\rangle$ and has the purity 0.999 955. After receiving the Bell measurement outcome from Alice, Bob implements the unitary transformation on his qubit in the usual way but does not implement any noise. The left sides of the four panels in Fig. 2 show that in this case the teleportation fidelity decreases with increasing noise, as expected and going below the classical limit. Now, in the second part of the experiment, on Alice's side there is always a maximum duration of noise corresponding to the optical path difference $237.6\lambda_0$ with $\lambda_0 = 808$ nm, and Bob begins to increase the duration of noise on his side in stepwise manner. The results are displayed on the right sides of the four panels in Fig. 2. With an increasing amount of noise on Bob's side, the teleportation fidelity increases. Note that in all cases,

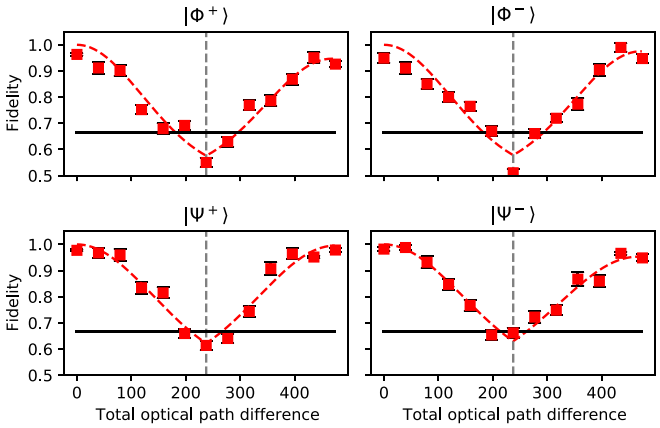

FIG. 2. The measured teleportation fidelity with error bars as a function of the amount of noise first on Alice's side followed by an increasing amount of noise on Bob's side. Vertical black lines indicate Alice's and Bob's sides for the noise. The dashed red curve is the theoretical fit for the experimental results including the possibly nonideal value of K [32]. The fits give an estimate of $-0.997 \leqslant K \leqslant -0.963$. The teleported input state is $\rho_{\text{in}} = \rho_+$ [Eq. (10)]. The results correspond to the first set of experimental results (see the text). The optical path difference is expressed in units of 808 nm. When Alice increases the noise on her side, the fidelity decreases. With an increasing amount of noise on Bob's side, the fidelity recovers. The horizontal black line indicates the classical limit of the fidelity with a value of $2/3$. Error bars are standard deviations calculated by the Monte Carlo method and mainly due to the counting statistics. In most cases, the error bars are smaller than the symbols.

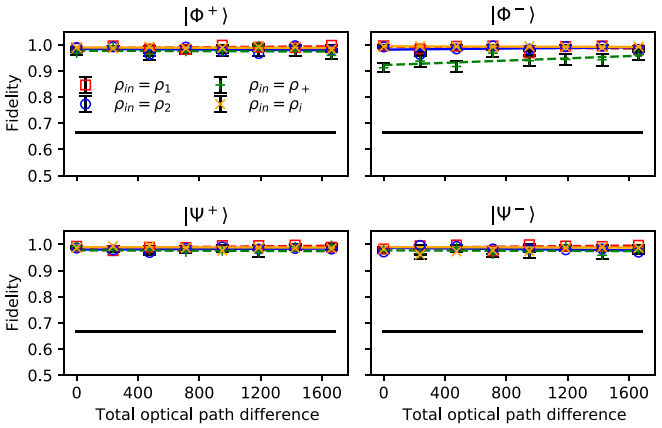

FIG. 3. The measured teleportation fidelity with error bars as a function of increasing and equal durations of noise on both Alice's and Bob's side. Teleported input states ρ_{in} are ρ_+ [Eq. (10)] (crosses), ρ_1 [Eq. (11)] (squares), ρ_2 [Eq. (12)] (circles), and ρ_i [Eq. (13)] (x's). Since the earlier fits, in Fig. 2, show that we are very close to the ideal case, the solid and dashed lines at the top are, for simplicity, linear fits for the experimental results. The results correspond to the second set of experimental results (see the text). The optical path difference corresponds to interaction time $t_a + t_b$ and is expressed in units of 808 nm. The fidelity remains essentially constant despite the presence of more and more noise. The horizontal black line near the bottom indicates the classical limit of the fidelity with a value of $2/3$. Error bars are standard deviations calculated by the Monte Carlo method and mainly due to the counting statistics. In most cases, the error bars are smaller than the symbols.

as well as for the results below, the experimental results for fidelity are based on performing state tomography also for the output state. When Bob has, in the last step, a maximum duration of noise corresponding to that on Alice's side, the high-fidelity values correspond to the case where there had essentially been no noise in any part of the protocol, i.e., the ideal teleportation efficiency is recovered. For example, for Bell measurement outcome $|\Psi^+\rangle$, the fidelity value without any noise (the first symbol in the lower-left panel in Fig. 2) is 0.978 ± 0.003, while the fidelity value with the maximum duration of noise on both sides (the last symbol in the lower-left panel in Fig. 2)] is 0.978 ± 0.006.

In the second experiment, the duration of the local noise on both Alice's and Bob's sides is increased in a stepwise manner, in equal steps on both sides. Figure 3 shows the results for four Bell measurement outcomes and using four different Alice states to be teleported. One of the input states is given by Eq. (10) and the other three, based on input state tomography, are

$$\rho_1 = \begin{pmatrix} 0.9794 & 0.0151 - i0.0321 \\ 0.0151 + i0.0321 & 0.0206 \end{pmatrix}, \quad (11)$$

$$\rho_2 = \begin{pmatrix} 0.0255 & 0.01304 + i0.0932 \\ 0.01304 - i0.0932 & 0.9745 \end{pmatrix}, \quad (12)$$

$$\rho_i = \begin{pmatrix} 0.6060 & 0.02178 - i0.4827 \\ 0.02178 + i0.4827 & 0.3940 \end{pmatrix}. \quad (13)$$

The purities of these states are 0.962 166, 0.968 013, and 0.989 419, respectively. When there is no noise at all (leftmost symbols in the panels in Fig. 3), high-fidelity teleportation is achieved, as expected. However, when there is an increasing duration of local noise on both sides, Alice's and Bob's, the fidelity does not decrease and remains essentially constant. For example with input state $\rho_{\text{in}} = \rho_i$ [Eq. (13)]and Bell measurement result $|\Psi^+\rangle$, the fidelity is 0.987 ± 0.002 without any noise and 0.985 ± 0.002 with the maximum duration of noise. This is a clear experimental demonstration that, even though there is hardly any entanglement left in the joint two-photon polarization state, one can in any case achieve high-fidelity teleportation when exploiting other useful resources available when considering also other degrees of freedom and the environment of an open system.

V. DISCUSSION AND CONCLUSIONS

We have realized experimentally a scheme for high-fidelity teleportation with dephasing noise. Here, a pair of entangled qubits—which initially contain the quantum resource for the protocol—is actually an open quantum system in which each of the qubits interacts with its local environment. Without the steps of the teleportation protocol, the dynamics of this bipartite open system displays non-Markovian features when the local environments of the qubits are initially correlated [14,31]. Note that there also exists a quantitative connection between the amount of non-Markovianity and the teleportation fidelity [32]. Therefore, we have demonstrated experimentally that it is possible to implement high-fidelity teleportation via a non-Markovian open quantum system.

Our results also show that it is no longer necessary for the original quantum resource to reside in the degrees of freedom or in the open system which are explicitly used in the original protocol—as long as useful resources still exist within or in the combination with the environment of the open system. It is also noteworthy here that in the described teleportation scheme, Alice's photon is destroyed in her Bell measurement, while at this point Bob has not yet done anything with his qubit. Despite this fact, Bob's subsequent open system qubit dynamics is influenced by the correlations initially existing between the two photons, even though Alice's photon no longer exists. In a sense, in addition to teleporting a qubit state, the protocol allows us to engineer in a nonlocal manner—both in time and in location—the open system dynamics of Bob's qubit.

In general, we have reported fundamental experimental results combining concepts from open quantum systems and quantum information. So far, there exists a number of sophisticated experiments which, e.g., implement reservoir engineering, quantum simulate Markovian open system dynamical maps, and control Markovian–to–non-Markovian transition and decoherence (see, e.g., [10–12,35]). However, very little is known or has been fundamentally tested when going beyond the traditional open system-environment setting and combining the open system dynamics with sophisticated quantum information protocols or other well-known quantum physical or optical schemes including, e.g., interferometry. We hope that our current results stimulate further work in this direction and help to explore new areas of quantum physics where open quantum systems, and their study, are used outside their traditional framework.

ACKNOWLEDGMENTS

This work was supported by the National Key Research and Development Program of China (Grant No. 2017YFA0304100), the National Natural Science Foundation of China (Grants No. 62005263, No. 11774335, No. 11821404, No. 11874345) Key Research Program of Frontier Sciences, CAS (Grant No. QYZDY-SSW-SLH003), the Fundamental Research Funds for the Central Universities (Grant No. WK2470000026), the Science Foundation of the CAS (Grant No. ZDRW-XH-2019-1), the Anhui Initiative in Quantum Information Technologies (Grant No. AHY020100), and the Science and Technological Fund of Anhui Province for Outstanding Youth (Grant No. 2008085J02). Z.D.L acknowledges financial support from the China Postdoctoral Science Foundation (Grant No. 2020M671862). S.H.R. acknowledges financial support from the Finnish Cultural Foundation and Turku University Foundation. J.P. acknowledges financial support from the Magnus Ehrnrooth Foundation.

[1] H.-P. Breuer and F. Petruccione, *The Theory of Open Quantum Systems* (Oxford University Press, Oxford, UK, 2007).
[2] Á. Rivas and S. F. Huelga, *Open Quantum Systems* (Springer, New York, 2012).
[3] D. Suter and G. A. Alvarez, Rev. Mod. Phys. **88**, 041001 (2016).
[4] Á. Rivas, S. F. Huelga, and M. B. Plenio, Rep. Prog. Phys. **77**, 094001 (2014).
[5] H.-P. Breuer, E.-M. Laine, J. Piilo, and B. Vacchini, Rev. Mod. Phys. **88**, 021002 (2016).
[6] I. de Vega and D. Alonso, Rev. Mod. Phys. **89**, 015001 (2017).
[7] L. Li, M. J. W. Hall, and H. M. Wiseman, Phys. Rep. **759**, 1 (2018).
[8] C.-F. Li, G.-C. Guo, and J. Piilo, Europhys. Lett. (Europhys. Lett.) **127**, 50001 (2019).
[9] C.-F. Li, G.-C. Guo, and J. Piilo, Europhys. Lett. (Europhys. Lett.) **128**, 30001 (2019).
[10] C. J. Myat, B. E. King, Q. A. Turchette, C. A. Sackett, D. Kielpinski, W. M. Itano, C. Monroe, and D. J. Wineland, Nature **403**, 269 (2000).
[11] B.-H. Liu, L. Li, Y.-F. Huang, C.-F. Li, G.-C. Guo, E.-M. Laine, H.-P. Breuer, and J. Piilo, Nature Physics **7**, 931 (2011).
[12] Z. D. Liu, H. Lyyra, Y.-N. Sun, B.-H. Liu, C.-F. Li, G.-C. Guo, S. Maniscalco, and J. Piilo, Nature Commun. **9**, 3453 (2018).
[13] A. Chiuri, C. Greganti, L. Mazzola, M. Paternostro, and P. Mataloni, Sci. Rep. **2**, 968 (2012).
[14] B.-H. Liu, D.-Y. Cao, Y.-F. Huang, C.-F. Li, G.-C. Guo, E.-M. Laine, H.-P. Breuer, and J. Piilo, Sci. Rep. **3**, 1781 (2013).
[15] F. F. Fanchini, G. Karpat, B. Cakmak, L. K. Castelano, G. H. Aguilar, O. J. Farias, S. P. Walborn, P. H. Souto Ribeiro, and M. C. de Oliveira, Phys. Rev. Lett. **112**, 210402 (2014).
[16] N. K. Bernardes, A. Cuevas, A. Orieux, C. H. Monken, P. Mataloni, F. Sciarrino, and M. F. Santos, Sci. Rep. **5**, 17520 (2015).
[17] B.-H. Liu, X.-M. Hu, Y.-F. Huang, C.-F. Li, G.-C. Guo, A. Karlsson, E.-M. Laine, S. Maniscalco, C. Macchiavello, and J. Piilo, Europhys. Lett. **114**, 10005 (2016).
[18] S. Cialdi, M. A. C. Rossi, C. Benedetti, B. Vacchini, D. Tamascelli, S. Olivares, and M. G. A. Paris, Appl. Phys. Lett. **110**, 081107 (2017).
[19] S. Yu *et al.*, Phys. Rev. Lett. **120**, 060406 (2018).
[20] A. Cuevas, A. Geraldi, C. Liorni, L. D. Bonavena, A. De Pasquale, F. Sciarrino, V. Giovannetti, and P. Mataloni, Sci. Rep. **9**, 3205 (2019).
[21] S. A. Uriri, F. Wudarski, I. Sinayskiy, F. Petruccione, and M. S. Tame, Phys. Rev. A **101**, 052107 (2020).
[22] J. F. Haase, P. J. Vetter, T. Unden, A. Smirne, J. Rosskopf, B. Naydenov, A. Stacey, F. Jelezko, M. B. Plenio, and S. F. Huelga, Phys. Rev. Lett. **121**, 060401 (2018).
[23] Y.-N. Lu, Y.-R. Zhang, G.-Q. Liu, F. Nori, H. Fan, and X.-Y. Pan, Phys. Rev. Lett. **124**, 210502 (2020).
[24] M. Wittemer, G. Clos, H.-P. Breuer, U. Warring, and T. Schaetz, Phys. Rev. A **97**, 020102(R) (2018).
[25] N. K. Bernardes, J. P. S. Peterson, R. S. Sarthour, A. M. Souza, C. H. Monken, I. Roditi, I. S. Oliveira, and M. F. Santos, Sci. Rep. **6**, 33945 (2016).
[26] D. Khurana, B. K. Agarwalla, and T. S. Mahesh, Phys. Rev. A **99**, 022107 (2019).
[27] Y. Dong *et al.*, npj Quantum Info. **4**, 3 (2018).
[28] C. H. Bennett, G. Brassard, C. Crèpeau, R. Jozsa, A. Peres, and W. K. Wootters, Phys. Rev. Lett. **70**, 1895 (1993).

[29] J.-G. Ren *et al.*, Nature **549**, 70 (2017).
[30] T. M. Graham, H. J. Bernstein, T.-C. Wei, M. Junge, and P. G. Kwiat, Nature Commun. **6**, 7185 (2015).
[31] E.-M. Laine, H.-P. Breuer, J. Piilo, C.-F. Li, and G.-C. Guo, Phys. Rev. Lett. **108**, 210402 (2012); **111**, 229901 (2013).
[32] E.-M. Laine, H.-P. Breuer, and J. Piilo, Sci. Rep. **4**, 4620 (2014).
[33] Y.-H. Kim, Phys. Rev. A **67**, 040301(R) (2003).
[34] F. Verstraete and H. Verschelde, Phys. Rev. Lett. **90**, 097901 (2003).
[35] P. Schindler *et al.*, Nat. Phys. **9**, 361 (2013).